


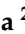


Article

Promoting the Flexibility of Thermal Prosumers Equipped with Heat Pumps to Support Power Grid Management

Giuseppe Edoardo Dino ^{1,2}, Pietro Catrini ^{1,*}, Valeria Palomba ², Andrea Frazzica ²
and Antonio Piacentino ¹

¹ Department of Engineering, University of Palermo, 90128 Palermo, Italy

² CNR ITAE, Salita S. Lucia sopra Contesse 5, 98126 Messina, Italy

* Correspondence: pietro.catrini@unipa.it

Abstract: The increasing share of renewable energy sources in energy systems will lead to unpredictable moments of surplus/deficit in energy production. To address this issue, users with heat pumps can provide support to power grid operators through flexible unit operation achieved via Demand Response programs. For buildings connected to low-temperature heating networks with ensured third-party access, further room for flexibility can be explored by investigating the production of surplus heat that can be sold to the network. A key aspect lies in the identification of the energy pricing options that could encourage such flexible operation of a heat pump by “thermal prosumers”. To this aim, the present study investigates the impact of ad hoc variations in the electricity purchasing price through discounts or penalties included in the “network cost” component of the price on cost-effective operation of a heat pump connected to the thermal network. To discuss the effects of different pricing options in terms of increased flexibility, an office building located in Italy and equipped with a high-temperature heat pump is adopted as the case study. A heuristic profit-oriented management strategy of the heat pump is assumed, and dynamic simulations are performed. The results indicate that at current electricity prices, the heat pump operation is profitable both when supplying the heat to meet the building’s requirements and when producing surplus heat for sale to the thermal network. In addition, it is revealed that the penalties applied to the electricity purchasing price are effective in encouraging changes in the heat pump operation strategy, reducing its average production (the building increasingly relying on buying heat from the network) and the associated electricity consumption by 46.0% and 79.7% in the “light” and “severe” local power deficit scenarios, respectively.

Keywords: district heating network; renewable energy; heat pump; prosumer; flexibility; heat pricing



Citation: Dino, G.E.; Catrini, P.; Palomba, V.; Frazzica, A.; Piacentino, A. Promoting the Flexibility of Thermal Prosumers Equipped with Heat Pumps to Support Power Grid Management. *Sustainability* **2023**, *15*, 7494. <https://doi.org/10.3390/su15097494>

Academic Editor: Mohamed A. Mohamed

Received: 10 March 2023

Revised: 21 April 2023

Accepted: 27 April 2023

Published: 3 May 2023



Copyright: © 2023 by the authors. Licensee MDPI, Basel, Switzerland. This article is an open access article distributed under the terms and conditions of the Creative Commons Attribution (CC BY) license (<https://creativecommons.org/licenses/by/4.0/>).

1. Introduction

Climate change and the recent energy crisis have raised the urgent need to increase the share of renewable energy sources (RESs) in the energy sector [1]. In this regard, in 2021, the Climate Change Conference (COP26) reaffirmed the role of RESs in achieving the Paris Agreement’s goal of limiting the global average temperature rise [2]. Regarding energy security, in the REPowerEU plan, the European Union raised the renewable target for 2030 to 45% as a strategy to reduce energy dependency from Russia [3]. However, the large exploitation of RESs has led to the development not only of new energy conversion systems [4] but also of new models of energy sharing such as renewable energy communities [5]. Indeed, it is widely recognized that new energy-sharing strategies can contribute greatly to reducing carbon dioxide emissions and energy waste [5]. However, to achieve these goals, technical and economic problems must still be solved [6]. For instance, the sharp increase of the RES capacity in the electricity sector observed in recent decades has raised the issue of unpredictable surplus and deficit of electricity production. In this regard, different solutions have been proposed to deal with these moments. For example, some

authors proposed solutions based on electricity storage [7,8], the management of the user demand [9], or power-to-X technologies [10,11]. Regarding the latter, the idea of using electricity from RESs for non-electric purposes allows the coupling of the electricity sector with other sectors, such as transportation, gas distribution, chemical industries, and heating and cooling networks [12,13]. Focusing on power-to-heat technologies, heat pumps (HPs) are considered valid support for transmission or distribution system operators (TSOs and DSOs) in managing excess electricity in the grid [14]. Indeed, through the provision of Demand Response (DR) programs, HPs could help TSOs in the moments of high surplus or deficit of electricity production [15]. More specifically, HPs could be activated for electricity overproduction, and the produced heat (not consumed by the user) could be stored on-site in the building envelope or in other storage systems [16].

Large efforts have been devoted by researchers to the investigation of HP capabilities to improve building operational flexibility. For instance, Zhang et al. [17] called attention to the need to define metrics for assessing building-to-grid flexibility achieved through HPs, by considering the different purposes of the involved actors (i.e., grid operators, final consumers, etc.). Meesenburg et al. [18] found that in the case of flexibility provision through HPs, higher exergy destruction during plant operation is observed, with a consequent increase in the final unit cost of the supplied heat. Lee et al. [19] performed a review of HP controls for providing ancillary services to the grid. The authors distinguished the capability of HPs to provide service for a load following reserve or frequency regulation. The authors identified that HPs could provide a better flexibility while guaranteeing reduced heat costs and higher ramp rates than other technologies, although the lack of experimental studies was pointed out. Manner et al. [20] investigated the capability of internet-connected residential HPs to provide primary frequency regulation. The authors found that only if residential HPs are aggregated, a sufficient capacity for primary frequency regulation is achieved. Bartolucci et al. [21] showed that in the case of electric microgrids, HPs coupled to thermal storage could provide ancillary service while assuring cost savings of up to 30%. Tina et al. [22] investigated the capability of commercial buildings in providing flexibility to help the TSO. A Mediterranean shopping center served by an HP was assumed as a case study, with two DR strategies compared. The authors found that a large flexibility potential exists throughout the year, although occupants' discomfort could arise during summer. For large-scale HPs, Meesenburg et al. [23] showed that they could provide primary frequency capacity. Arteconi and Polonara [24] investigated the capability of an air-source HP coupled to an underfloor heating system to provide flexibility through DR. The authors implemented HP control based on the electricity price, which decreases (or increases) the HP temperature set point depending on high or low electricity market price. A substantial decrease in the peak demand was achieved. Vivian et al. [25] found that HPs coupled to thermal energy storage in a residential district could contribute to reducing stress on the power grid. Ibrahim et al. [26] developed a dynamic model of a variable speed HP for providing frequency regulation support. The authors provided a detailed state-space model of the HPs. Rasmussen et al. [27] developed an algorithm for the activation of large-scale HPs for primary frequency support. The authors found that the strategy tends to increase the overall energy consumption but allows a better operation of the power system reducing the peak demand. Rodríguez et al. [28] compared different strategies for implementing DR by using HPs in plus-energy dwellings. The authors found that a proper combination of variable temperature setpoints and dynamic electricity pricing could lead to 15% of cost savings. Gjorgievski et al. [29] reviewed existing projects focused on DR via power-to-heat technologies. The authors pointed out that direct load control of power-to-heat technologies is more effective than real-time pricing requiring a quick response. Other studies developed sophisticated controls for DR in buildings via HP [30,31]. You et al. [32] evaluated the operational flexibility of residential HPs, taking into account heat demand uncertainties. Schibuola et al. [33] compared three control strategies for DR through an HP coupled with a solar thermal plant and a photovoltaic system. Two of them relied on the hourly electricity prices, and one was based on HP activation using

only electricity produced by the photovoltaic panels. The last strategy allowed for cost reduction and energy savings. Research has also considered the possibility of using district heating networks (DHN) for the storage of surplus heat produced by distributed HPs [34]. It is worth noting that, in this case, the user connected to the DHN could act for certain hours either as a heat consumer or producer (termed the “thermal prosumer”) similarly to the option with the electricity grid [35]. Research focused on the integration of HPs into DHNs has covered a broad spectrum of studies: from solving technical issues (e.g., different operating temperatures [36], pressure imbalance due to the presence of multiple heat producers [37]) to the lack of a proper pricing mechanism [38] or a well-established regulatory framework [39]. Regarding the regulatory framework, the concept of “third-party access” (TPA) has also been extended from the electrical grids to the DHNs. In general, regardless of the heat sources (e.g., thermal RESs, HPs, and industry), economic and policy conditions should be provided to grant access to new heat suppliers to the DHN [40]. It is recognized that TPA facilitates higher competition (and consequently the efficiency) of heat production, and reduction of greenhouse gas emissions [41]. Some projects have also considered TPA for solar thermal prosumers in DHNs [42,43]. Finally, the effects of energy pricing on the integration of heat supplied by distributed producers with HPs have been investigated. For instance, Østergaard et al. [44] highlighted the importance of taxes in the electricity and heat prices in promoting the increase of the capacity of the distributed HPs in the DHNs. Dominković et al. [45] investigated dynamic pricing for DHN systems in the presence of multiple producers. The authors found that the inclusion of HPs could lead to a lower marginal heat cost and reduced carbon dioxide emissions.

The previous literature review pointed out that numerous published papers have recently investigated the capability of users with HPs to support the grid operators in the times of surplus/deficit of electricity from RESs [46]. However, most studies investigate strategies for promoting the operational flexibility of the HPs not connected to DHNs, with a primary focus on small-capacity units supplying heat to a single dwelling or a small group of energy users with either a fixed or stochastic load. To the authors’ knowledge, there is an apparent literature gap regarding the operational flexibility of distributed heat pumps connected to DHNs with room for increased the HP operational flexibility due to the possibility of selling excess heat to the network. At present, such a configuration becomes of particular interest because of the relevant role recognized by energy communities in the transition toward sustainable energy. Additional novelty of such strategy is in the perspective adopted in this study with respect to energy pricing: in most of the published literature, the HP operational flexibility is investigated by assuming a given energy price profile according to a typical “price taker” approach; in this paper, however, the potential effects of discounts or penalties applied to the electricity prices are investigated, thus also rendering the results of potential interest for policy making. In line with this goal, a reference arrangement involving an HP connected to a low-temperature DHN with a third-party access option is considered, which qualifies the building as a thermal prosumer capable of gaining revenues from selling the heat. The economic boundary conditions (e.g., the purchasing prices of electricity and heat) and technical constraints (e.g., temperature and pressure setpoints of the DHN) must be taken into account, since they affect the operation and profit of thermal prosumers [44,47]. Focusing on the economic conditions, the present study investigates the effects of ad hoc changes in the electricity purchasing prices on the operational flexibility of a thermal prosumer with an HP and coupled to a DHN. More specifically, this study will assess whether a change in the component of the electricity price related to the “power grid management and support to the energy system” could be:

- A useful strategy for TSOs and DSOs to promote operational flexibility of thermal prosumers so that they could be of help in the times of surplus and deficit of electricity supplied from RESs. It is worth noting that no change has been imposed in the current management of the electricity or heat market.
- An opportunity for a typical heat consumer with an HP and connected to the DHN to become a thermal prosumer. Indeed, the unit cost of heat produced by HPs will be

highly sensitive to the electricity purchasing prices, and this cost will affect the user's decision to self-produce heat or buy it from the DHN (in case of thermal demand), and finally, the possibility of being a heat producer when excess heat is produced on-site [48].

To show the energy and economic benefits of the proposed strategy, an office building located in Northern Italy supplied by an HP and connected to a DHN is adopted as the case study. A profit-oriented heuristic algorithm for HP operation is developed. The analysis is based on a validated model of the prosumer's substation in the DHN, and an annual dynamic simulation is performed in the Transient System Simulation Studio (TRNSYS). Energy savings and economic revenues will be calculated and compared to a reference scenario characterized by the adoption of the DHN as the only heat source for meeting the user's thermal demand. The analysis considers some alternative scenarios based on different variations in the electricity purchasing prices.

This paper is structured as follows. In Section 2, the algorithm for HP operation is presented. In Section 3, the case study is described together with the modeling. In Section 4, the results are presented and discussed. In Section 5, the last section, conclusions are briefly drawn.

2. Materials and Method

Before providing details on the strategy proposed for promoting the operational flexibility of a thermal prosumer, a description of the management of HP is given.

2.1. Description of the Profit-Oriented Heat Pump Management Strategy

To perform this analysis, it is necessary to preliminary define a management strategy for the HP installed in the prosumer's substation. In this respect, a thermal prosumer aims at maximizing its profit by operating the HP depending on the economic boundary conditions (i.e., electricity and heat purchasing price). Figure 1 shows a profit-oriented heuristic management strategy for the HP in the prosumer's substation, considering the economic (i.e., prices) and technical conditions. For each time step (typically, one hour), the strategy evaluates if it is profitable to activate the HP only for self-production or for selling heat to DHN, or to switch it off and use the DHN as the only heat source. Figure 1 shows three economic conditions that can affect the HP operation (as indicated by the yellow parallelograms in the figure). The first two are the buying/selling prices of heat from/to DHN, here indicated as p_{h,DHN_buy} and p_{h,DHN_sell} , respectively. The third parallelogram is the electricity buying price ($p_{e,buy}$). This price significantly contributes to the unit cost of heat produced on site by the HP, i.e., $c_{h,HP}$. However, it is worth noting that $c_{h,HP}$ depends on technological aspects as well. Indeed, the HP coefficient of performance (COP), controls, and interface with the substation, highly affect the amount of electrical energy required by the HP. As the first step, the measured T_{air} and the part-load ratio (indicated as PLR and expressed as the ratio of the user demand, D_h , and the HP heating capacity, H_c) are used as input data for the HP model to calculate the COP (see Equation (1)).

$$COP = f(T_{air}, PLR) \quad (1)$$

The unit cost of the heat produced by the HP is then calculated by using the COP (from Equation (1)) and the price of the electricity purchased from the grid, as shown in Equation (2).

$$c_{h, HP} = p_{e, buy} COP \quad (2)$$

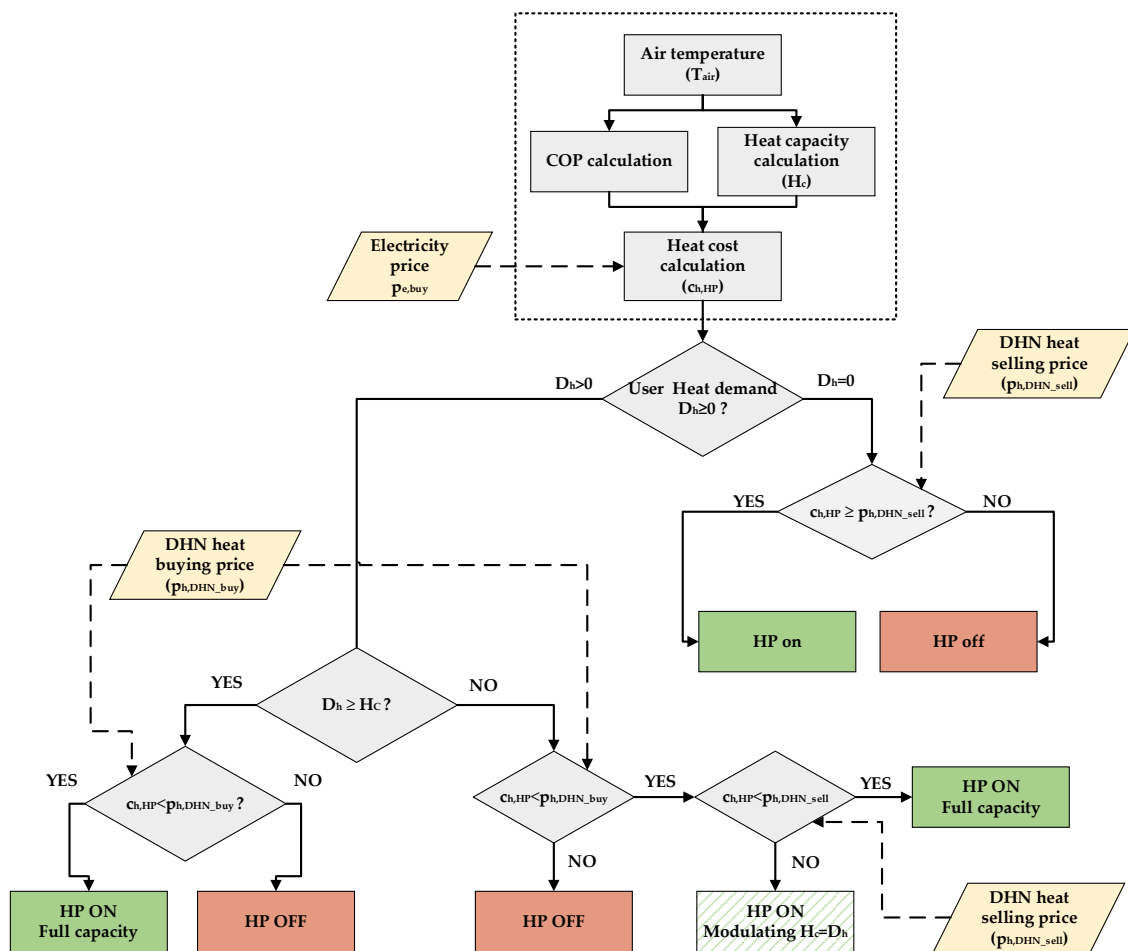


Figure 1. Flowchart of the profit-oriented management strategy of a thermal prosumer with an HP (Grey boxes: reading and calculation steps; yellow boxes: introduction of economic conditions; red and green boxes: output of the strategy).

In the presence of a heat demand (i.e., $D_h \neq 0$), the algorithm suggests the most profitable HP operation strategy. In particular:

- When the user's thermal demand is higher than the HP heating capacity (i.e., $D_h > H_c$), if the unit cost of heat produced by the HP, $c_{h,HP}$ is greater than the heat purchasing price, then the HP is switched off, and the prosumer meets its demand by using heat from the DHN. Conversely, if the unit cost of heat produced by the HP is lower than the heat purchasing price, the HP is operated at "full capacity", and the uncovered fraction of the thermal demand (i.e., $D_h - H_c$) is met by using heat from the DHN.
- When the demand is lower than the HP heating capacity (i.e., $D_h < H_c$), if the cost of heat produced by the HP is higher than the heat purchasing price, the HP is switched off, and the prosumer meets its thermal demand by using the heat from the DHN. A reverse situation in this case requires a further distinction. Indeed, since $D_h < H_c$, it is necessary to understand if it is profitable to run the HP only to cover the user demand (i.e., modulating its capacity), or to run the HP at its full capacity and sell the surplus heat to the DHN. More specifically, as shown in Figure 1, if the unit cost of the heat produced by the HP is greater than the heat selling price, the HP is modulated to run at full capacity.

In the case of null heat demand from the user (i.e., $D_h = 0$), the strategy evaluates whether it is profitable to sell the heat to the network by comparing the unit cost of the heat produced by the HP and the heat selling price.

Lastly, it is worth pointing out that although most studies have analyzed the HP operational flexibility using optimization methods [47,49], the adoption of a heuristic approach could be justified by the fact that this study does not aim to find an optimal HP management strategy for flexibility provision, but rather it assesses the sensitivity of the profit gained by the prosumer from the ad hoc changes in the electricity purchasing prices.

2.2. Description of the Strategy for Promoting the Flexibility of a Thermal Prosumer

Different components are usually found in electricity purchasing prices. These components are related to energy production, management of the power grid, and taxes. In this study, to promote the operational flexibility of thermal prosumers with HPs, the component of the price of the electricity related to the “network costs” and “energy system support” (briefly indicated as $p_{e,buy}^{NC\&ES}$) was varied while keeping the component related to the energy generation cost $p_{e,buy}^{GEN}$ fixed.

To quantify the effects of this strategy on the profit of the thermal prosumer, different scenarios were proposed. As shown in Figure 2, the “Neutral” scenario is characterized by the absence of incentives or penalties aimed at promoting the user’s operational flexibility. For the other scenarios, a transition was assumed from a “Severe Deficit” in electricity production from RESs (during the whole year) to a constant “Severe Surplus” condition characterized by a large availability of electricity from RESs. In the “Surplus” scenarios (i.e., both “severe” and “light”), HPs could help the TSO by increasing its electricity consumption with the heat produced, consumed on site, or sold to the DHN. Conversely, in the “Deficit” scenarios, the TSO could encourage the users with HPs to decrease electricity consumption. In general, in the case of a severe deficit on the supply side, a rise in the electricity price is the strategy pursued by the TSO to encourage the users to decrease their consumption. Contrarily, in the case of severe surplus, a lower electricity price encourages the users to increase energy consumption. As shown in Figure 2, for scenarios of “deficit” in electricity production (red circles in the figure), an increase in $p_{e,buy}^{NC\&ES}$ was assumed (+100% for the “Severe Deficit” and +60% for the “Light Deficit”). Inversely, for scenarios of “surplus” in electricity production (green triangles in the figure), a discount in $p_{e,buy}^{NC\&ES}$ was assumed (−100% for the “Severe Surplus” and −60% for the “Light Surplus”).

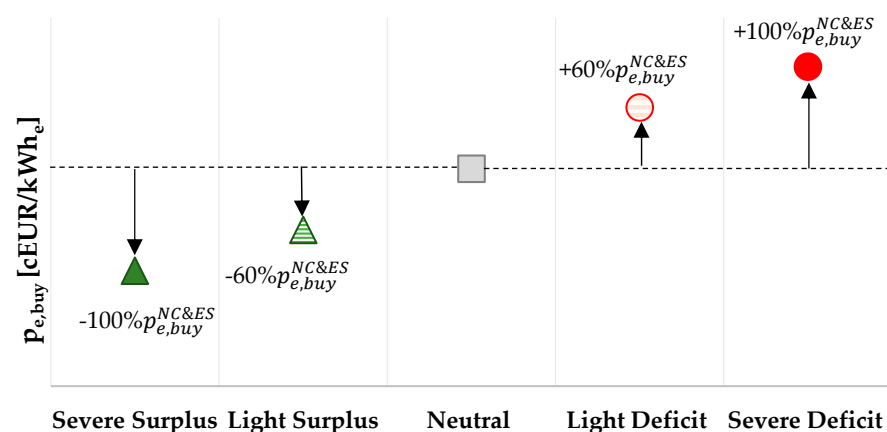


Figure 2. Variation of the electricity buying price in each scenario.

Two more scenarios (not shown in Figure 2) were investigated. More specifically, in both, a “random” variation (on an hourly basis) in the electricity price was assumed. As shown in Equation (3), in the “Random1” scenario, the electricity buying price randomly varied between the value of the electricity buying price in the “Severe Surplus” scenario (i.e., $p_{e,buy,min}^{SevSur}$) and that of the “Severe Deficit” scenario (i.e., $p_{e,buy,max}^{SevDef}$), thus replicating unpredictable moments of electricity deficit and surplus.

In the second case, termed the “Random2” scenario, the electricity buying price values (i.e., $p_{e,buy}^{RAND2}$) varied as shown in Equation (4). In particular, starting from the “Random1”

scenario, the following constraints were imposed: (i) if the electricity price $p_{e,buy}^{RAND1}$ is lower than the maximum value of the “Neutral” scenario, then $p_{e,buy}^{RAND2}$ was assumed equal to $p_{e,buy}^{RAND1}$; (ii) if the electricity price $p_{e,buy}^{RAND1}$ is higher than the maximum value of the “Neutral” scenario, then $p_{e,buy}^{RAND2}$ was assumed equal to $p_{e,buy,MAX}^{NEUT}$ (Equation (4)). Compared to the “Random1” scenario, “Random2” scenario assumes electricity price variation to help the TSO only in the hours of electricity deficit (i.e., “Severe Deficit” or “Light Deficit” situations). Conversely, the electricity price does not vary in the hours of electricity surplus. However, the reason for this choice will be better clarified in the result section.

$$p_{e,buy}^{RAND1} = p_{e,buy,min}^{SevSur} \leq RANDOM \leq p_{e,buy,MAX}^{SevDef} \quad (3)$$

$$p_{e,buy}^{RAND2} = \begin{cases} p_{e,buy}^{RAND1} & \text{IF } p_{e,buy}^{RAND1} \leq p_{e,buy,MAX}^{NEUT} \\ p_{e,buy,MAX}^{NEUT} & \text{IF } p_{e,buy}^{RAND1} > p_{e,buy,MAX}^{NEUT} \end{cases} \quad (4)$$

3. Description of the Case Study and Investigated Scenarios

An office building located in Verona Villafranca (Veneto, Northern Italy) with a maximum thermal demand equal to 75 kW was adopted as the case study. The user’s heat demand profile was obtained by using the Building Energy Signature method [50,51]. This approach allows for developing the hourly distribution of the building’s thermal demand D_h as shown in the following equation:

$$D_h(i) = D_{h,des} \cdot \left[\frac{T_{H,LET} - T_{air}(i)}{T_{H,LET} - T_{des}} \right] \quad (5)$$

where $D_{h,des}$ is the design heat load of the building calculated at the outdoor design temperature T_{des} , T_{air} is the dry bulb temperature of the outdoor air, $T_{H,LET}$ is the outdoor air temperature at which the net heat load of the building is equal to zero. In this analysis, $T_{H,LET}$ was set at 20 °C as suggested by [52], and $D_{h,des}$ was set to 75 kW (maximum thermal demand of the user). By knowing the values for T_{air} , the hourly distribution of D_h and the total energy request for the considered period were calculated. A further load related to domestic hot water (DHW) demand was considered. The DHW demand is shown in Table 1. The overall hourly thermal power and monthly energy requests (comprehensive of heating and DHW demand) are shown in Figure 3. The global annual energy demand is equal to 63.3 MWh.

Table 1. Daily schedule for DHW production.

Daily Hours	Temperature Set Point	Hourly Heat Capacity
10–12 (3 h)	55 °C	11.03 kW
15–16 (2 h)	55 °C	11.03 kW

The weather file of Verona Villafranca (Cfa climate according to Köppen classification) was retrieved from the METEONORM database [53].

3.1. Description and Modeling of the Prosumer’s Substation

Figure 4 shows a schematic of the prosumer substation adopted in this work. This arrangement was based on the experimental setup proposed by Pipiciello et al. in [54]. In recent work, Dino et al. [55] developed a virtual model of this substation in TRNSYS 18, which was duly validated by using data available from [54].

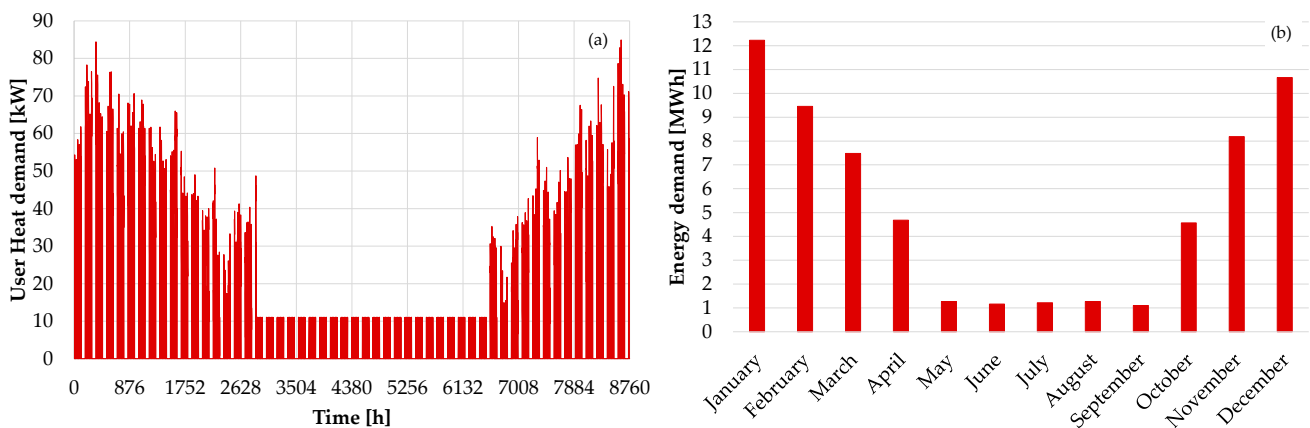


Figure 3. Data of the case study: (a) hourly heat demand of the user and (b) monthly energy demand.

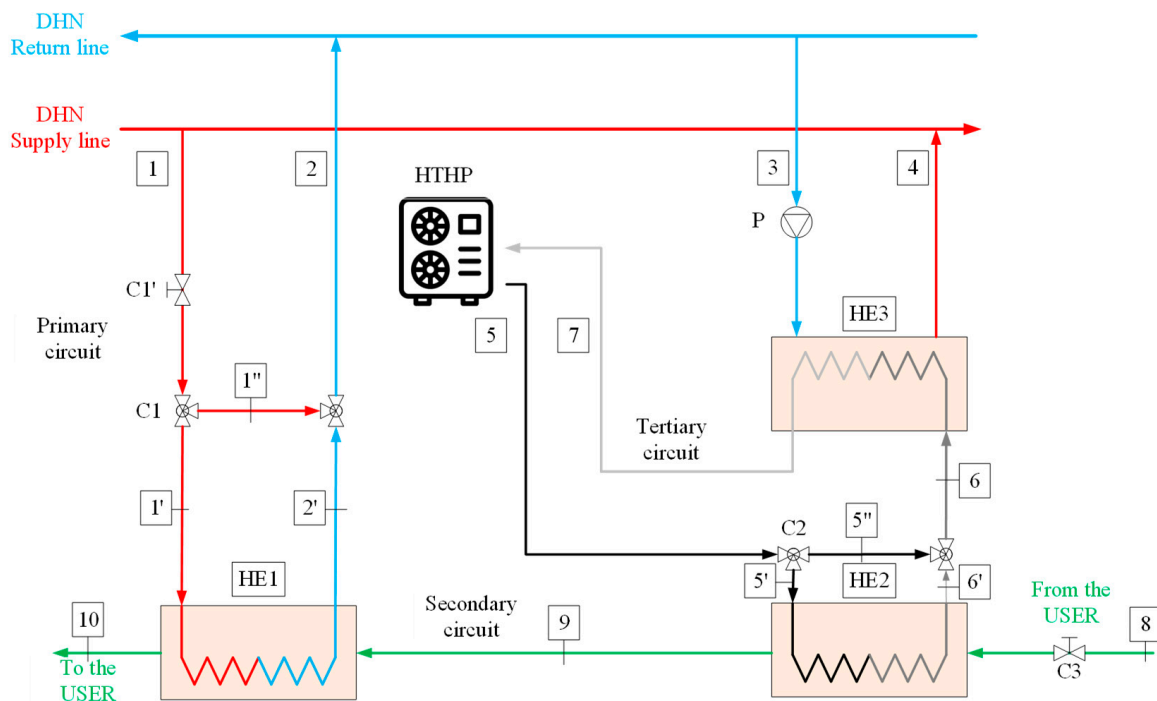


Figure 4. Schematic of the thermal prosumer's substation.

As shown in Figure 4, a “return-to-supply” configuration of the substation was assumed. It includes three heat exchangers (HEs) and a High-Temperature Heat Pump (HTHP). A variable water flow rate is drawn from the return line of the DHN and heated up using HE3 to the supply temperature setpoint (i.e., 60 °C) by the HTHP. The water flow rate returning from the hydronic loop of the building is heated using heat from the HTHP via HE2. Then, if the supply water temperature is not equal to the setpoint required by the user, the water flow rate is heated via HE1 using heat available from the DHN.

Three different circuits are then identified as follows:

1. The primary circuit which directly connects the DHN to the substation. It includes the accessories used when the user is either a producer or consumer (i.e., HE1 and HE3). It is activated to cover the user energy demand if HE2 cannot supply the overall energy amount requested (through HE1), or when the heat generated by HTHP is exchanged with DHN (through HE3).
2. The secondary circuit, which consists of the HE1, HE2, and other accessories, used to heat the water returning from the hydronic loop of the building.

3. The tertiary circuit, where the heat produced by the HTHP is exchanged with the water returning from the building through HE2 and with the DHN via HE3.

In the present study, a 4th generation DHN was assumed. For this reason, the operating temperature of the supply line of the DHN was equal to 60 °C. Details on temperature, flow rates, and HE sizes, are reported in Table 2.

Table 2. Design parameters for the heat exchanger installed with the substation.

	Primary Side		Secondary Side	
Heat Exchanger HE1	F1'	7.30 m ³ /h	F9	4.87 m ³ /h
	T1'	60 °C	T9	40 °C
	T2'	50 °C	T10	55 °C
	Q		85 kW	
	UA		11.77 kW/°C	
Heat Exchanger HE2	F5'	3.65 m ³ /h	F8	4.87 m ³ /h
	T5'	70 °C	T8	40 °C
	T6'	50 °C	T9	55 °C
	Q		85 kW	
	UA		6.89 kW/°C	
Heat Exchanger HE3	F3	1.93 m ³ /h	F6	2.41 m ³ /h
	T3	35 °C	T6	70 °C
	T4	60 °C	T7	50 °C
	Q		56 kW	
	UA		4.54 kW/°C	

As previously mentioned, the described system was reproduced in the TRNSYS environment [55]. The HE modeling followed the same approach as in [55]. More specifically, Type5 (counter-flow heat exchanger) was used and the overall heat exchanger coefficient was externally calculated by considering an empirical correlation obtained by an elaboration of the Dittus–Boelter equation. The HP management strategy was implemented in TRNSYS by using a “calculator”, which provides the operating signal for the HTHP. Iterative feedback controllers (type 22) were adopted to simulate the controls that regulate valves C2, C1, and the speed of pump P (Figure 4). They attempt to maintain the required temperature set point by varying the flow delivered to the heat exchangers (HE1 for C1 and HE2 for C2) or the flow rate delivered by the pump P (for HE3). A detail of the iterative feedback controller settings is shown in Table 3.

Table 3. Iterative feedback controller settings.

Actuator Device	Controlled Variable	Temperature Setpoint
C1	T ₁₀	55 °C
C2	T ₉	55 °C
P	T ₄	60 °C

Finally, C1' and P control the flow rate on the hot side of HE1 and cold side of HE3, respectively, according to the control logic shown in Table 4.

Table 4. Settings Value for the flow rate control.

Actuator Device	Controlled Variable	Control Logic
C1'	F ₂	C1' is open if T ₉ < 55 °C AND F ₈ > 0
P	F ₃	P is activated if T ₆ ≥ 65 °C AND F ₇ > 0

In conclusion, it is worth stressing the main assumptions of this work. First, the hydraulic modeling of the whole DHN was not included, and for this reason, constraints related to pressure setpoint, and the maximum flow rate of the hot water that could be

injected into the DHN by the prosumer were accounted for. Secondly, the analysis did not consider any constraints related to the operation of the DHN, e.g., the actual request from the DHN of the surplus heat produced in loco by the prosumer. All these aspects affect the operation of distributed thermal prosumers [47]. In this work, the DHN was assumed as a virtual storage, whose operation is not influenced by the capacity of the considered prosumer. However, this assumption could be no more justified for a larger heating capacity of the prosumer, or if an optimization in the management of HP should be carried out [47].

3.2. Modelling of the High-Temperature Heat Pump

Considering the temperature of the hot water supplied to the hydronic loop of the user (i.e., 55 °C) and the operating temperature of the DHN (i.e., 60 °C), it was necessary to select an air-to-water HP capable of producing hot water at 70 °C. A “KWP” high-temperature heat pump, provided by Kroll[®] (Germany) was selected [56]. In Table 5, the main technical data are summarized. Figure 5 shows the heating capacity and the COP values for the case of hot water produced at $T_{water} = 70$ °C. Note that the profiles shown in the referenced figure consider only the variation in the COP and heating capacity with the temperature of the air entering the evaporator (i.e., T_{air}). Conversely, the effect of part-load operation was not provided.

Table 5. Technical data of the selected HTHP.

Working area	
$T_{air} > -15$ °C	$35 < T_{water} \leq 70$ °C
Refrigerant	
R32 Filling quantity: 22 kg GWP = 675	R1234ze Filling quantity: 5 kg GWP = 7
Compressor	
Scroll compressor Maximum operating current: 25.7 A Maximum power consumption: 15.5 kW	Reciprocating compressor Maximum operating current: 33.2 A Maximum power consumption: 19 kW

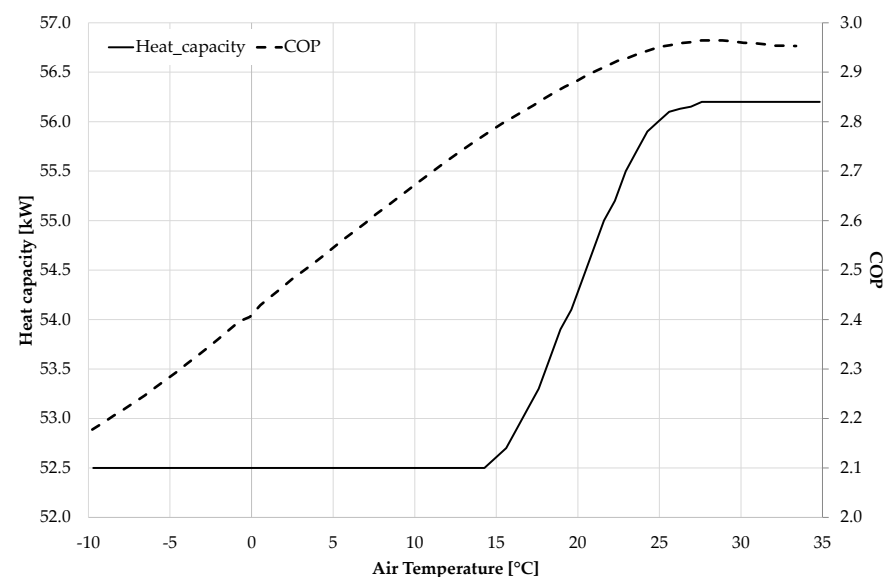


Figure 5. HTHP performance curves evaluated for $T_{water} = 70$ °C [56].

The data retrieved from the datasheet were processed in a statistical model to obtain equations that allow for a quick calculation of the performance of the HTHP by knowing only T_{air} , while keeping the temperature of the produced hot water at 70 °C. It is worth not-

ing that this “black-box” approach is very useful, for instance, for embedding experimental or empirical data in algorithms that make use of Model Predictive Controls [57]. Moreover, the approach relies on polynomial equations which usually require a low computational effort while guaranteeing good approximation [58–60].

Following this method, a non-linear regression analysis was carried out to correlate T_{air} with COP and heating capacity. A MATLAB script was used to obtain two sets of predictors for the non-linear polynomial equations that describe the HTHP performance in the following form:

$$H_C = p_1 \times T_{air}^4 + p_2 \times T_{air}^3 + p_3 \times T_{air}^2 + p_4 \times T_{air} + p_5 \quad (6)$$

$$COP = p_6 \times T_{air}^4 + p_7 \times T_{air}^3 + p_8 \times T_{air}^2 + p_9 \times T_{air} + p_{10} \quad (7)$$

The heating capacity, H_C is expressed in kW, the T_{air} in °C. The predictor coefficients and the statistical evaluation parameters are shown in Table 6. High values of R^2 (close to 1) and low values of root mean square error (RMSE) show the predictor’s reliability. In Figure 6, the comparison between the datasheet and calculated performance is reported showing the good correspondence of the black box model.

Table 6. Values of predictors and evaluation parameters of the statistical regression.

	$H_C(15^\circ\text{C} < T_{air} < 27.5^\circ\text{C})$		COP
p_1	1.563×10^{-4}	p_6	-4.450×10^{-9}
p_2	-1.591×10^{-2}	p_7	-1.210×10^{-5}
p_3	0.574	p_8	1.068×10^{-4}
p_4	-8.466	p_9	2.628×10^{-2}
p_5	96.13	p_{10}	2.412
R^2	0.9992		0.9998
SSE	0.406		7.421×10^{-4}
RMSE	0.0395		3.353×10^{-3}
$H_C(-10^\circ\text{C} \leq T_{air} \leq 15^\circ\text{C})$			
52.5 kW			
$H_C(T_{air} \geq 27.5^\circ\text{C})$			
56.2 kW			

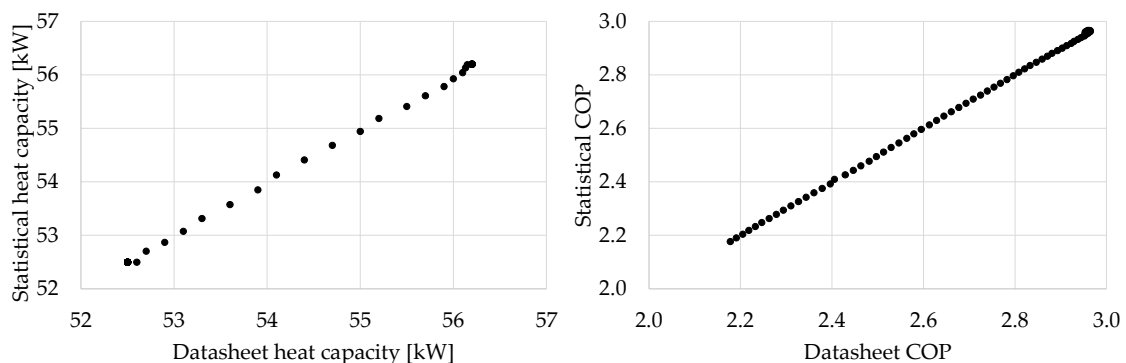


Figure 6. Comparison of data retrieved from datasheet with statistically predicted data.

The HTHP equations (Equations (6) and (7)) were implemented in the TRNSYS model by using a “calculator”. The profit-oriented strategy for the assumed HTHP did not consider the possibility of modulating the HP heating capacity (i.e., the possibility of operating the HTHP at PLR values between 0 and 1), as only full-load data were available from the manufacturer. The outlet temperature of the water on the condenser is set at 70 °C, and the difference between the inlet and outlet temperature is set at 20 K. Since the heating capacity

and COP depend only on T_{air} , the flow rate is assumed variable and is calculated through the following expression:

$$\dot{m}_{cond} = \frac{H_C}{c_p \Delta T} (\Delta T = 20 \text{ K}) \quad (8)$$

3.3. Description of the Economic Boundary Conditions

In this subsection, the heat and electricity prices for the case study are shown. Regarding the heat price, the substation was considered a part of a DHN with one main distributor that imposes the buying price, and the TPA is allowed with a fixed buying and selling heat price for the prosumer.

To account for real market heat prices, data of heat purchasing prices released by DHN distribution company in Veneto during 2021 were adopted. In particular, the prices for non-household customers who consume less than 29 MWh per month were used [61]. Since in the real case there are no prosumers, the selling price offered by the distributor to the prosumer was assumed to be 80% of the buying price (Table 7) based the average ratio between buying and selling price reported in [62].

Table 7. Reference value for heat purchasing price (from DHN to the prosumer) and heat selling price (from the prosumer to the DHN).

Heat Price	1 Jan.–1 Apr.	1 Apr.–1 Jul.	1 Jul.–1 Oct.	1 Oct.–31 Dec.
$p_{H, DHN, buy}$ (EUR/kWh)	0.0965	0.1009	0.1168	0.1554
$p_{H, DHN, sell}$ (EUR/kWh)	0.0772	0.0807	0.0934	0.1243

Data available from the Italian Agency for Energy Market Regulation (ARERA) were used for the electricity price [63]. More specifically, the Italian electricity price for both 2021 semesters and a non-household consumer with an installed power are assumed greater than 15 kW_e (Table 8). As shown in Table 8, data from ARERA showed a clear picture of the components of the electricity price related to energy production, the management of the power grid, and taxes.

Table 8. Reference value of the purchasing price of electricity.

Period	Energy Generation Cost Component $p_{e, buy}^{GEN}$ (EUR/kWh)	Network Cost and Energy System Support Component $p_{e, buy}^{NC\&ES}$ (EUR/kWh)	Final Price (VAT and Taxes Included) (EUR/kWh)
2021, 1st semester	0.0736	0.0613	0.1771
2021, 2nd semester	0.1218	0.0396	0.2094

Based on the electricity prices shown in Table 8, the prices for the investigated scenarios (see Figure 2) were calculated as shown in Table 9. The prices vary between 0.1157 EUR/kWh and 0.2491 EUR/kWh. Moreover, the analysis considers a variation of the electricity prices for two semesters in one year.

Table 9. Variation in the electricity purchasing price for the first five scenarios.

Period	“Severe Deficit” (+100% $p_{e, buy}^{NC\&ES}$) (EUR/kWh)	“Light Deficit” (+60% $p_{e, buy}^{NC\&ES}$) (EUR/kWh)	“Neutral” (No Variation) (EUR/kWh)	“Light Surplus” (−60% $p_{e, buy}^{NC\&ES}$) (EUR/kWh)	“Severe Surplus” (−100% $p_{e, buy}^{NC\&ES}$) (EUR/kWh)
2021, 1st semester	0.2384	0.2139	0.1771	0.1403	0.1157
2021, 2nd semester	0.2491	0.2332	0.2094	0.1856	0.1698

3.4. Description of the Adopted Economic Indicators

For each scenario, a cash flow (CF) was calculated as the difference between revenues arising from the heat selling and costs sustained for purchasing heat from DHN and electricity from the grid (Equation (9)). The calculation of revenues and costs was performed on an hourly basis and for one-year operation (Equations (10) and (11)). The unit heat prices are reported in Table 7 and considered constant for each scenario, while the adopted electricity prices are shown in Table 9.

$$CF = M_{revenues} - M_{costs} \quad (9)$$

$$M_{revenues} = \sum_{\tau=1}^{8760} E_{th,HE3}(\tau) \times p_{h,DHN_{sell}}(\tau) \quad (10)$$

$$M_{costs} = \sum_{\tau=1}^{8760} E_{th,HE1}(\tau) \times p_{h,DHN_{buy}}(\tau) + E_{el}(\tau) \times p_{e,buy}(\tau) \quad (11)$$

To better understand the economic benefits achievable in each scenario, a baseline scenario characterized by the absence of an HTHP was assumed. In particular, in this scenario, the thermal energy demand of the user is entirely met by the heat supplied by the DHN, bringing the one-year cost to 7210 EUR. As shown in Equation (12), this cost leads to a negative cash flow, since no revenues are generated in this scenario.

$$CF_{base} = 0 - \sum_{\tau=1}^{8760} D_h(\tau) \times p_{h,DHN_{buy}}(\tau) \quad (12)$$

Arising from this outcome, the one-year economic savings were then calculated by the difference between the cash flows achieved in each scenario and the baseline one (Equation (13)).

$$SAV_{ref} = CF_{scenario} - CF_{base} \quad (13)$$

Finally, the economic savings were also calculated by comparing the “Neutral” scenario with the other scenarios (Equation (14)). This information is useful to compare the same technological system under different boundary economic conditions due to the flexible operation.

$$SAV_{neut} = CF_{scenario} - CF_{neutral} \quad (14)$$

4. Results and Discussion

To assess the energy savings and the economic benefits achievable by the thermal prosumer, it is worth analyzing the results obtained from a one-year simulation.

Figure 7 shows the amount of energy exchanged in all HEs after one year of operation. These results are useful to gain insights into the effect of the strategy here proposed on the operation of the HTHP and the substation (e.g., interactions among the HEs, and between the substation and the DHN). It is worth noting that HE2 (orange bars in Figure 7) shows a constant amount of energy exchanged for each of the proposed scenarios, except for the “Severe Deficit” scenario. Conversely, the amount of thermal energy exchanged in HE3 (grey bars) shows an increasing trend when moving from the “Severe Deficit” to the “Severe Surplus” scenario. This trend could be easily explained by the fact that due to the decreasing electricity price, the HTHP is operated for a longer period with more thermal energy available for the DHN.

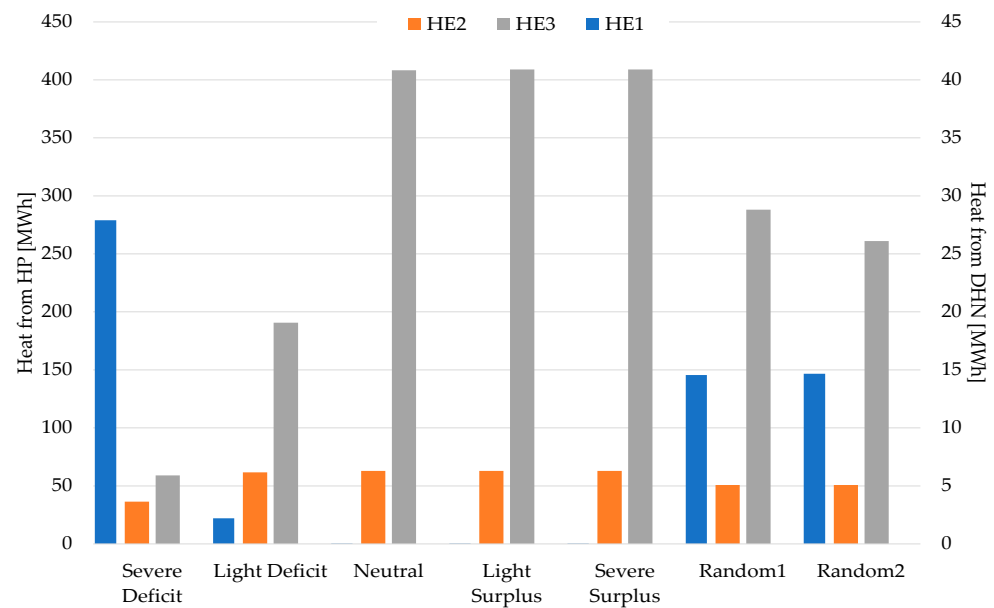


Figure 7. Thermal energy exchanged within each heat exchanger (values for HE2 and HE3 are on the left axis, HE1 on the right).

In almost all the scenarios, the thermal demand of the user is almost covered by using HE2 (i.e., by using the energy supplied by the HTHP) as evidenced by the energy exchanged in HE1 (blue bars) which is always less than 0.05 MWh. For the “Severe Deficit” and “Light Deficit” scenarios, the energy exchanged in HE1 is not zero, and it is equal to 27.9 MWh and 2.2 MWh, respectively. Both values account for 44% and 3.5% of the heat consumed by the user in one year. The “Random1” and “Random2” scenarios show equal values of heat exchanged by HE1 and HE2 (i.e., 14.6 MWh and 50.7 MWh). In addition, the energy exchanged by HE3 in the “Random2” scenario is lower than the one of the “Random1”.

A focus on the amount of heat exchanged by the three HEs is shown in Figure 8. More specifically, the results are presented only for the two opposite scenarios, i.e., “Severe Deficit” and “Severe Surplus”. Comparing Figure 8a,b, the heat rate for HE1 and HE2 is equal, since both HEs operate to meet the energy demand on the user side. HE3 is never activated in the “Severe Deficit” scenario, while it operates for 8 h at a constant heat transfer rate in the “Severe Surplus” scenario. The different behavior is due to more profitable economic conditions in the “Severe Surplus” scenario, which encourage the prosumer to activate the HTHP for selling heat to the DHN. However, as shown in Figure 8b, HE3 is operated in the absence of energy demand by the user, i.e., during evening, nighttime, and early morning. Note that, as already mentioned, this analysis did not consider any constraints on the maximum amount of heat that could be supplied by the prosumer to the DHN during nighttime.

Figure 9 shows the electrical energy supplied to the HTHP for one-year operation. Following the criterion shown in Section 2, it is apparent that the electrical energy consumed by the HTHP in one year decreases in scenarios of higher electricity prices. Indeed, moving from the “Light Deficit” scenario to “Severe Deficit”, the electricity consumed by the HTHP decreased from 92 MWh in the “Light Deficit” (−46.0% compared to the “Neutral” scenario) to 35 MWh (−79.7% compared to the “Neutral” scenario) in the “Light Deficit”. For the “Random1” and “Random2” scenarios, energy consumption was 123 MWh and 110 MWh. In particular, both scenarios show intermediate results between the “Light Deficit” and “Neutral” scenarios, even though they were characterized by different boundary conditions. The observed trend justified that changes in the electricity prices could promote the operational flexibility of the user.

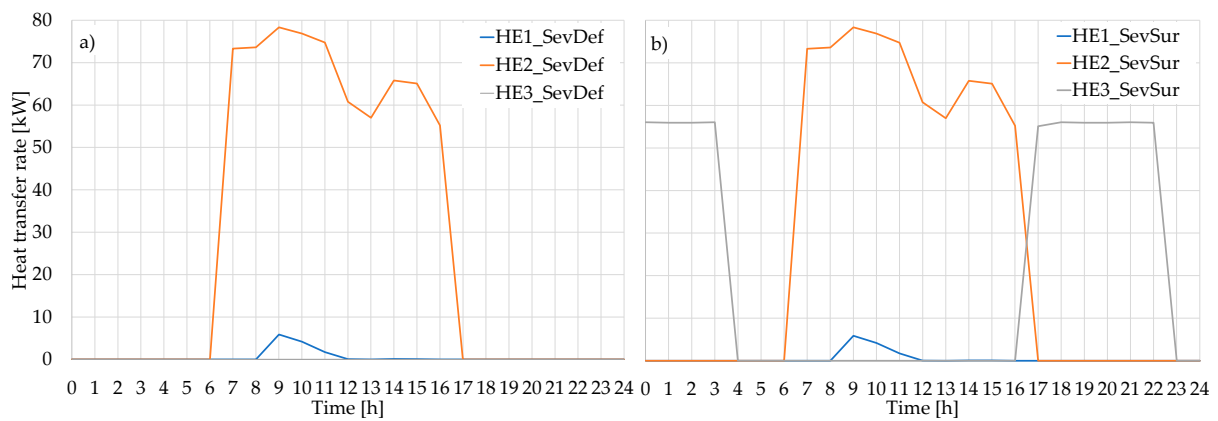


Figure 8. Substation's heat transfer rate daily trend: (a) "Severe Deficit" scenario; (b) "Severe Surplus" scenario.

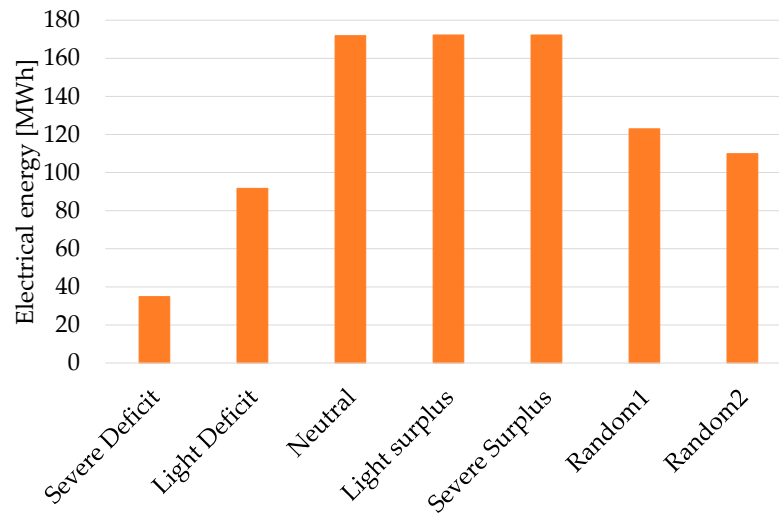


Figure 9. Electrical energy supplied to the HTHP.

As previously mentioned, the economic analysis considered the savings from the thermal energy produced by the HTHP (which is no longer purchased from the DHN) and the revenues from the thermal energy sold to the DHN. The annual economic cash flows and savings reported in Figure 10a were calculated assuming as a baseline scenario the one with no HTHP installed and the DHN used as the only heat source. The annual economic cash flows and savings reported in Figure 10b were calculated adopting the "Neutral" scenario as the reference (i.e., when the HTHP is installed but with no variation in the electricity prices). As shown in Figure 10a, the cash flow and savings show an increasing trend when moving from the "Severe Deficit" scenario to the "Severe Surplus" scenario, due to the decreasing electricity price. Both CF and SAV_{base} are negative for the "Severe Deficit" scenario, thus suggesting that it would be more profitable to exploit the DHN as a heat source. Although in the "Light Deficit" scenario the cash flow is still negative, the savings are positive since it is referred to the baseline conditions with the entire demand covered by DHN and no heat selling. As shown in Figure 10b, money savings are achieved only in scenarios of electricity surplus and in "Random1".

The "Random1" scenario achieved economic performance similar to that of the "Neutral" scenario. The "Random2" scenario achieved a cash flow close to zero but a SAV_{base} equal to 6763 EUR, thus suggesting that it is profitable to include the HTHP. In Figure 10b, the "Severe Deficit" and "Light Deficit" scenarios show negative results since they are referred to as the neutral scenarios. This is due to the less profitable conditions imposed by the electrical grid operator. Conversely, the "Light Surplus" and "Severe Surplus" sce-

narios achieved positive values of SAV_{neut} ; the results range between $-10,359$ EUR and $18,493$ EUR. For the “Random1” and “Random2” scenarios, a counterintuitive result is achieved: indeed, the energetic outcomes showed that the performances of these scenarios were intermediate between the “Light Deficit” and “Neutral” scenarios, while the economic results show that they are closer to the “Neutral” one. This is due to the random distribution of electricity prices that affect the HTHP activation and the economic balances with different effects.

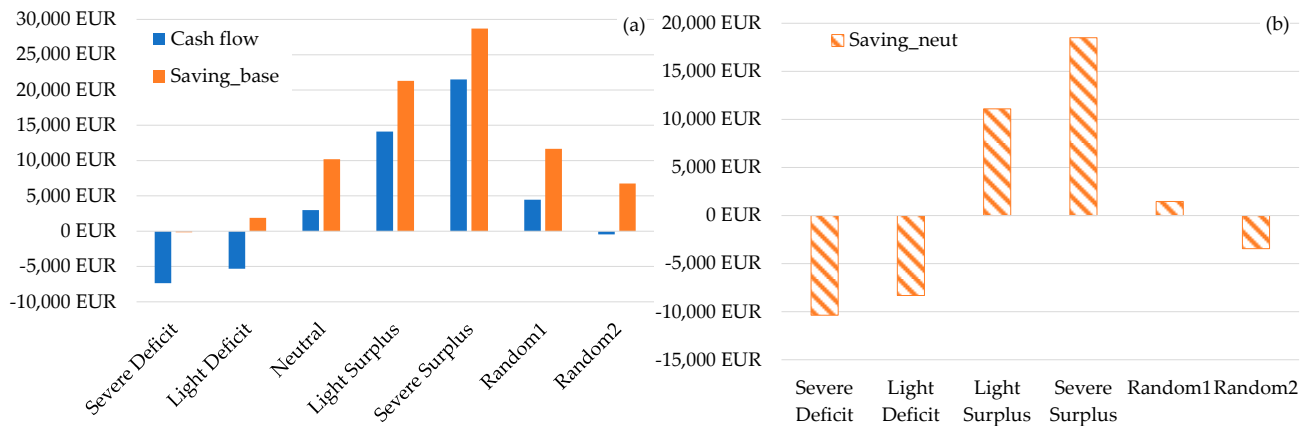


Figure 10. Cash flow and money savings for each scenario: (a) with no HTHP and (b) adopting the “Neutral” scenario as the reference.

The analysis of the described results revealed that in the “Neutral” scenario, profitable results can be achieved, compared to the DHN used as the only heat source.

The introduction of discounts for promoting operational flexibility during electricity surplus leads to a relevant increase in profit. If such a strategy is carried out using public resources, the effect is an extra profit generated by the system that is already profitable without taxation or incentives (i.e., in the “Neutral” scenario). If public incentives aim at balancing inequalities, discounts may, on the contrary, lead to a significant increase. The “Random1” scenario considers the whole range of prices; therefore, less profitable conditions are offset by the more convenient ones.

From the previous findings, the “Random2” scenario was developed. It was conceived by cutting off all the values of prices that could increase the profit. Then, electricity prices are varied taking into account only penalties when the grid used as the only heat source (i.e., “Severe Deficit” or “Light Deficit” situations). Despite this penalization, the results shown in Figure 10 let us appreciate the positive results achieved by this case due to the performance of the HTHP.

To better understand the energetic and economic results shown here, it is worth comparing the annual profile of the unit cost of heat produced by an HP with the buying and selling price of heat from the DHN. Figure 11a shows that the unit cost of heat in the “Severe Deficit” scenario is comparable with the purchasing price of heat from the DHN (black continuous line vs. pink line), thus suggesting that on-site heat production does not always provide cost savings. Regarding the selling price of heat (black dashed line), the profiles shown in Figure 11a indicate that only the “severe” and “light” deficit scenarios have hours characterized by no benefits from selling heat to the DHN. Conversely, economic benefits are achieved through the sale of heat to the DHN in the other scenarios.

In scenarios “Random1” and “Random2”, the unit cost of heat shows an oscillating behavior, which, in the first scenario, allows for more profitable conditions than those of the second scenario (Figure 11b,c).

Development of a Prediction Model of the Unit Cost of Heat

The previous analysis highlighted that the economic boundary conditions together with HP energy performance highly affect the operation and profit of the thermal prosumer.

Moreover, as previously mentioned, there is not always a match between favorable market conditions and good HP performance. It is interesting to find a correlation between the unit cost of heat and the boundary conditions (i.e., the outdoor temperature affects the HP energy performance and the market price of electricity). It is worth noting that other operating and marginal costs (e.g., maintenance costs) are here neglected, but they can be easily included in the methodology.

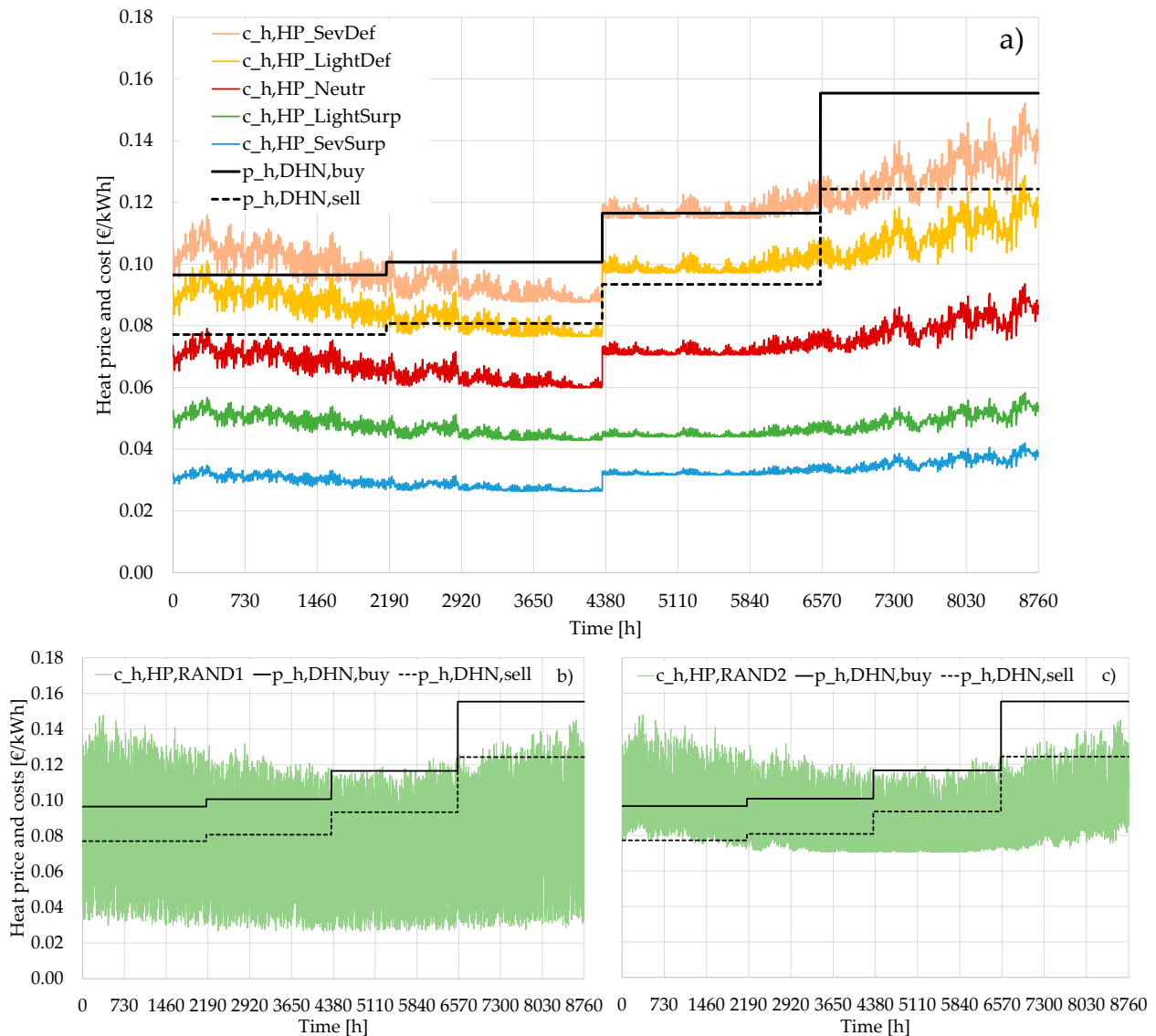


Figure 11. Comparison between DHN heat buying and selling price and the unit cost of heat produced by the HTHP for: (a) scenarios obtained by varying the NC and ES electricity price components, (b) “Random1” scenario, (c) “Random2” scenario.

To find a correlation between c_h , T_{air} , and p_{el} , the results of the simulation were used as input for a statistical regression in the MATLAB model. The results of regression analysis suggested that the unit cost of heat is related to T_{air} and p_{el} according to the polynomial equation shown in Equation (15). The values of predictors are shown in Table 10, together with the statistical evaluation parameters.

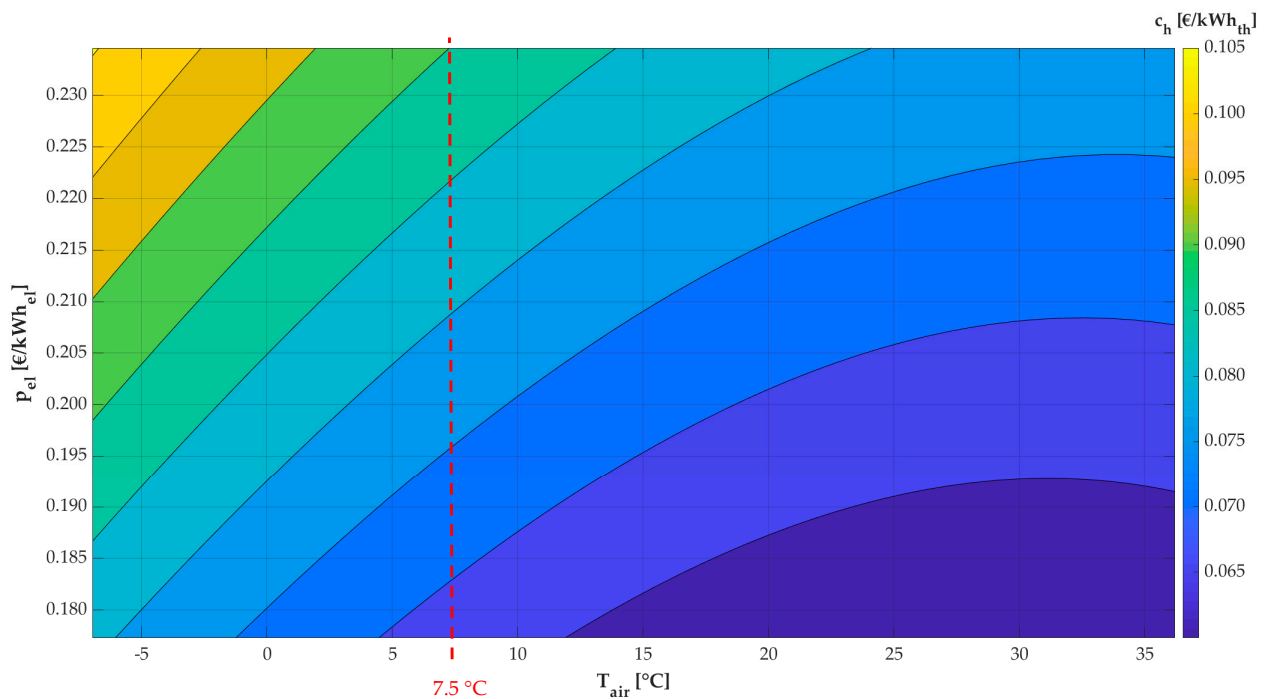
$$c_h = a_0 + a_1 \times T_{air} + a_2 \times p_{el} + a_3 \times T_{air}^2 + a_4 \times T_{air} \times p_{el} \quad (15)$$

Table 10. Values of the statistical predictors and evaluation parameters.

Predictor	
a_0	1.978×10^{-3}
a_1	-4.490×10^{-4}
a_2	4.053×10^{-1}
a_3	1.557×10^{-5}
a_4	-2.701×10^{-3}
Predictor evaluation parameter	
R ²	0.0017
SSE	0.9994
RMSE	1.850×10^{-4}

Such a black box model allows for fast and reliable heat costing and can be directly integrated into an evaluation tree algorithm such as the one proposed in this paper. Indeed, Equation (15) predicts the cost of heat generated on-site by the HTHP with the known values T_{air} , p_{el} from the weather forecast and market conditions imposed by the grid dealer.

The regression model of Equation (15) was also presented in the form of a “map”, as shown in Figure 12. Such representation allows us to assess the sensitivity of the unit cost of heat to the electricity prices and outdoor air temperature. More specifically, when $T_{air} < 7.5$ °C, c_h is highly sensitive to the electricity prices p_{el} , as evidenced by the rapid change of colors in the contour plot (region to the left of the red dashed line). For temperature values higher than 7.5 °C, conversely, the sensitivity of c_h to the electricity prices is greatly reduced (region to the right from the dashed line).

**Figure 12.** Map of the unit cost of heat.

5. Conclusions

The present work investigated the behavior of a thermal prosumer with an HP when changes in the components of the electricity purchasing price are adopted as a strategy to increase its operational flexibility. More specifically, this study analyzed the effects of discounts and penalties included in the component related to the “power grid management and support to the energy system”. A thermal prosumer’s substation equipped with an HTHP and servicing an office building in Northern Italy was adopted as the case study.

Dynamic simulations for one-year operation were performed using a TRNSYS model developed by the authors in the past work. A profit-oriented heuristic management strategy for the HP operation was developed and implemented in the dynamic simulations. Seven different scenarios were investigated, each one related to different economic conditions imposed by the TSOs and DSOs to promote the prosumer's operational flexibility. The analysis revealed that the ad hoc changes in the electricity purchasing price (either discounts or penalties) are a good strategy for promoting operational flexibility. For instance, in the case of "light" and "severe" electricity deficits from RESs, the penalties applied to the electricity purchasing price appear effective in encouraging a change in the heat pump operational strategy, reducing its average production and the associated electricity consumption by 46.0% and 79.7%, respectively. Moreover, the results of the economic analysis showed that with current electricity and heat prices, heat pump operation is profitable for both meeting the building's thermal needs and producing heat for sale to the DHN. However, discounting the electricity prices during electricity surplus led to a substantial increase in the prosumer's profit. This outcome highlighted the fact that a thorough analysis of discounts is necessary to avoid unjustified incentives, especially when public resources are used. Future studies should focus on thermal grids with substations that include different local heat generators, with a special focus on those supplied using by RES technologies. The substation performance will be analyzed taking into account the constraints related to the DHN architecture, the capability of the network to consume the heat provided by prosumers, and the coordination of the DR programs for heat and electricity. Finally, heat pricing methods and third-party access regulatory framework will be also included to support the decision by policymakers in developing renewable energy communities.

Author Contributions: Conceptualization, G.E.D., P.C. and A.P.; methodology, G.E.D., P.C. and A.P.; software, G.E.D.; validation, G.E.D.; investigation, G.E.D. and P.C.; resources, A.F. and V.P.; data curation, G.E.D.; writing—original draft preparation, G.E.D. and P.C.; writing—review and editing, A.F. and V.P.; visualization, A.F. and V.P.; supervision, A.P. All authors have read and agreed to the published version of the manuscript.

Funding: This study was developed in the framework of the research activities carried out within the PRIN 2020 project: "OPTIMISM—Optimal refurbishment design and management of small energy micro-grids", funded by the Italian Ministry of University and Research (MUR).

Institutional Review Board Statement: Not applicable.

Informed Consent Statement: Not applicable.

Data Availability Statement: Not applicable.

Conflicts of Interest: The authors declare no conflict of interest.

Nomenclature

Acronyms

DHN	District Heating Network
DR	Demand–Response system
DSO	Distribution System Operator
HE	Heat Exchanger
HP	Heat Pump
HTHP	High-Temperature Heat Pump
RESs	Renewable energy Sources
TSO	Transmission System Operator

Variables

CF	Cash flow (EUR)
$c_{h,HP}$	Cost of heat produced by the heat pump (EUR/kWh)
c_p	Specific heat (kJ/(kg °C))
E_{el}	Electrical energy (kwh or MWh)

E_{th}	Thermal energy (kWh or MWh)
H_c	Heating capacity (kW)
\dot{m}	Flow rate (kg/s)
$M_{revenues}$	Revenues (EUR)
M_{costs}	Costs (EUR)
$p_{e,buy}$	Electricity price (EUR/kWh)
p_{h,DHN_buy}	Price of heat bought from district heating network (EUR/kWh)
p_{h,DHN_sell}	Price of heat sold to district heating network (EUR/kWh)
R^2	R-squared—Coefficient of determination (dimensionless)
SSE	Sum of Squares Estimate of errors (kW)
RMSE	Root Mean Square Error (kW)
RAND	Random distribution function
\dot{Q}	Heat transfer rate (kW)
SAV	Economic Savings (EUR)
τ	Time (s or h)
UA	Global Heat transfer coefficient (kW/°C)

References

- Climate Change—Topics—IEA. Available online: <https://www.iea.org/topics/climate-change> (accessed on 13 February 2023).
- Guzović, Z.; Duić, N.; Piacentino, A.; Markovska, N.; Mathiesen, B.V.; Lund, H. Paving the Way for the Paris Agreement: Contributions of SDEWES Science. *Energy* **2023**, *263*, 125617. [[CrossRef](#)]
- Available online: https://Commission.Europa.Eu/Strategy-and-Policy/Priorities-2019-2024/European-Green-Deal/Repowereu-Affordable-Secure-and-Sustainable-Energy-Europe_en (accessed on 14 February 2023).
- Praveenkumar, S.; Agyekum, E.B.; Kumar, A.; Velkin, V.I. Thermo-Enviro-Economic Analysis of Solar Photovoltaic/Thermal System Incorporated with u-Shaped Grid Copper Pipe, Thermal Electric Generators and Nanofluids: An Experimental Investigation. *J. Energy Storage* **2023**, *60*, 106611. [[CrossRef](#)]
- Ceglia, F.; Marrasso, E.; Samanta, S.; Sasso, M. Addressing Energy Poverty in the Energy Community: Assessment of Energy, Environmental, Economic, and Social Benefits for an Italian Residential Case Study. *Sustainability* **2022**, *14*, 15077. [[CrossRef](#)]
- Krug, M.; di Nucci, M.R.; Caldera, M.; de Luca, E. Mainstreaming Community Energy: Is the Renewable Energy Directive a Driver for Renewable Energy Communities in Germany and Italy? *Sustainability* **2022**, *14*, 7181. [[CrossRef](#)]
- Bartolini, A.; Carducci, F.; Muñoz, C.B.; Comodi, G. Energy Storage and Multi Energy Systems in Local Energy Communities with High Renewable Energy Penetration. *Renew. Energy* **2020**, *159*, 595–609. [[CrossRef](#)]
- Kebede, A.A.; Kalogiannis, T.; Van Mierlo, J.; Berecibar, M. A Comprehensive Review of Stationary Energy Storage Devices for Large Scale Renewable Energy Sources Grid Integration. *Renew. Sustain. Energy Rev.* **2022**, *159*, 112213. [[CrossRef](#)]
- Alsokhry, F.; Siano, P.; Annuk, A.; Mohamed, M.A. A Novel Time-of-Use Pricing Based Energy Management System for Smart Home Appliances: Cost-Effective Method. *Sustainability* **2022**, *14*, 14556. [[CrossRef](#)]
- Thellufsen, J.Z.; Lund, H.; Sorknæs, P.; Østergaard, P.A.; Chang, M.; Drysdale, D.; Nielsen, S.; Djørup, S.R.; Sperling, K. Smart Energy Cities in a 100% Renewable Energy Context. *Renew. Sustain. Energy Rev.* **2020**, *129*, 109922. [[CrossRef](#)]
- Wulf, C.; Zapp, P.; Schreiber, A. Review of Power-to-X Demonstration Projects in Europe. *Front. Energy Res.* **2020**, *8*, 191. [[CrossRef](#)]
- Guelpa, E.; Bischi, A.; Verda, V.; Chertkov, M.; Lund, H. Towards Future Infrastructures for Sustainable Multi-Energy Systems: A Review. *Energy* **2019**, *184*, 2–21. [[CrossRef](#)]
- Lund, H. Renewable Heating Strategies and Their Consequences for Storage and Grid Infrastructures Comparing a Smart Grid to a Smart Energy Systems Approach. *Energy* **2018**, *151*, 94–102. [[CrossRef](#)]
- Bloess, A.; Schill, W.P.; Zerrahn, A. Power-to-Heat for Renewable Energy Integration: A Review of Technologies, Modeling Approaches, and Flexibility Potentials. *Appl. Energy* **2018**, *212*, 1611–1626. [[CrossRef](#)]
- Fischer, D.; Madani, H. On Heat Pumps in Smart Grids: A Review. *Renew. Sustain. Energy Rev.* **2017**, *70*, 342–357. [[CrossRef](#)]
- Le Dréau, J.; Heiselberg, P. Energy Flexibility of Residential Buildings Using Short Term Heat Storage in the Thermal Mass. *Energy* **2016**, *111*, 991–1002. [[CrossRef](#)]
- Zhang, L.; Good, N.; Mancarella, P. Building-to-Grid Flexibility: Modelling and Assessment Metrics for Residential Demand Response from Heat Pump Aggregations. *Appl. Energy* **2019**, *233–234*, 709–723. [[CrossRef](#)]
- Meesenburg, W.; Ommen, T.; Elmegaard, B. Dynamic Exergoeconomic Analysis of a Heat Pump System Used for Ancillary Services in an Integrated Energy System. *Energy* **2018**, *152*, 154–165. [[CrossRef](#)]
- Lee, Z.E.; Sun, Q.; Ma, Z.; Wang, J.; MacDonald, J.S.; Max Zhang, K. Providing Grid Services With Heat Pumps: A Review. *ASME J. Eng. Sustain. Build. Cities* **2020**, *1*, 011007. [[CrossRef](#)]
- Manner, P.; Alapera, I.; Honkapuro, S. Domestic Heat Pumps as a Source of Primary Frequency Control Reserve. In Proceedings of the International Conference on the European Energy Market, EEM, Stockholm, Sweden, 16–18 September 2020. [[CrossRef](#)]
- Bartolucci, L.; Cordiner, S.; Mulone, V.; Santarelli, M. Ancillary Services Provided by Hybrid Residential Renewable Energy Systems through Thermal and Electrochemical Storage Systems. *Energies* **2019**, *12*, 2429. [[CrossRef](#)]

22. Tina, G.M.; Aneli, S.; Gagliano, A. Technical and Economic Analysis of the Provision of Ancillary Services through the Flexibility of HVAC System in Shopping Centers. *Energy* **2022**, *258*, 124860. [CrossRef]
23. Meesenburg, W.; Markussen, W.B.; Ommen, T.; Elmegaard, B. Optimizing Control of Two-Stage Ammonia Heat Pump for Fast Regulation of Power Uptake. *Appl. Energy* **2020**, *271*, 115126. [CrossRef]
24. Arteconi, A.; Polonara, F. Assessing the Demand Side Management Potential and the Energy Flexibility of Heat Pumps in Buildings. *Energies* **2018**, *11*, 1846. [CrossRef]
25. Vivian, J.; Prataiviera, E.; Cunsolo, F.; Pau, M. Demand Side Management of a Pool of Air Source Heat Pumps for Space Heating and Domestic Hot Water Production in a Residential District. *Energy Convers. Manag.* **2020**, *225*, 113457. [CrossRef]
26. Ibrahim, I.; O'Loughlin, C.; O'Donnell, T. Virtual Inertia Control of Variable Speed Heat Pumps for the Provision of Frequency Support. *Energies* **2020**, *13*, 1863. [CrossRef]
27. Harild Rasmussen, T.B.; Wu, Q.; Zhang, M. Primary Frequency Support from Local Control of Large-Scale Heat Pumps. *Int. J. Electr. Power Energy Syst.* **2021**, *133*, 107270. [CrossRef]
28. Romero Rodríguez, L.; Sánchez Ramos, J.; Álvarez Domínguez, S.; Eicker, U. Contributions of Heat Pumps to Demand Response: A Case Study of a plus-Energy Dwelling. *Appl. Energy* **2018**, *214*, 191–204. [CrossRef]
29. Gjorgievski, V.Z.; Markovska, N.; Abazi, A.; Duić, N. The Potential of Power-to-Heat Demand Response to Improve the Flexibility of the Energy System: An Empirical Review. *Renew. Sustain. Energy Rev.* **2021**, *138*, 110489. [CrossRef]
30. Bechtel, S.; Rafii-Tabrizi, S.; Scholzen, F.; Hadji-Minaglou, J.-R.; Maas, S. Influence of Thermal Energy Storage and Heat Pump Parametrization for Demand-Side-Management in a Nearly-Zero-Energy-Building Using Model Predictive Control. *Energy Build.* **2020**, *226*, 110364. [CrossRef]
31. Péan, T.Q.; Salom, J.; Costa-Castelló, R. Review of Control Strategies for Improving the Energy Flexibility Provided by Heat Pump Systems in Buildings. *J. Process. Control.* **2019**, *74*, 35–49. [CrossRef]
32. You, Z.; Zade, M.; Kumaran Nalini, B.; Tzscheutschler, P. Flexibility Estimation of Residential Heat Pumps under Heat Demand Uncertainty. *Energies* **2021**, *14*, 5709. [CrossRef]
33. Schibuola, L.; Scarpa, M.; Tambani, C. Demand Response Management by Means of Heat Pumps Controlled via Real Time Pricing. *Energy Build.* **2015**, *90*, 15–28. [CrossRef]
34. Buffa, S.; Soppelsa, A.; Pipiciello, M.; Henze, G.; Fedrizzi, R. Fifth-Generation District Heating and Cooling Substations: Demand Response with Artificial Neural Network-Based Model Predictive Control. *Energies* **2020**, *13*, 4339. [CrossRef]
35. Zinsmeister, D.; Lickleder, T.; Christange, F.; Tzscheutschler, P.; Perić, V.S. A Comparison of Prosumer System Configurations in District Heating Networks. *Energy Rep.* **2021**, *7*, 430–439. [CrossRef]
36. Barco-Burgos, J.; Bruno, J.C.; Eicker, U.; Saldaña-Robles, A.L.; Alcántar-Camarena, V. Review on the Integration of High-Temperature Heat Pumps in District Heating and Cooling Networks. *Energy* **2022**, *239*, 122378. [CrossRef]
37. Nord, N.; Shakerin, M.; Tereshchenko, T.; Verda, V.; Borchellini, R. Data Informed Physical Models for District Heating Grids with Distributed Heat Sources to Understand Thermal and Hydraulic Aspects. *Energy* **2021**, *222*, 119965. [CrossRef]
38. Frölke, L.; Sousa, T.; Pinson, P. A Network-Aware Market Mechanism for Decentralized District Heating Systems. *Appl. Energy* **2021**, *306*, 117956. [CrossRef]
39. Bürger, V.; Steinbach, J.; Kranzl, L.; Müller, A. Third Party Access to District Heating Systems—Challenges for the Practical Implementation. *Energy Policy* **2019**, *132*, 881–892. [CrossRef]
40. Botsaris, P.N.; Giourka, P.; Papatsounis, A.; Dimitriadou, P.; Goitia-Zabaleta, N.; Patsonakis, C. Developing a Business Case for a Renewable Energy Community in a Public Housing Settlement in Greece—The Case of a Student Housing and Its Challenges, Prospects and Barriers. *Sustainability* **2021**, *13*, 3792. [CrossRef]
41. Gross, M.; Karbasi, B.; Reiners, T.; Altieri, L.; Wagner, H.J.; Bertsch, V. Implementing Prosumers into Heating Networks. *Energy* **2021**, *230*, 120844. [CrossRef]
42. SDH Project. Available online: <https://www.solar-district-heating.eu/> (accessed on 17 February 2023).
43. SDHp2m Project. Available online: <https://www.solar-district-heating.eu/sdhp2m-2/> (accessed on 17 February 2023).
44. Østergaard, P.A.; Andersen, A.N. Variable Taxes Promoting District Heating Heat Pump Flexibility. *Energy* **2021**, *221*, 119839. [CrossRef]
45. Dominković, D.F.; Wahlroos, M.; Syri, S.; Pedersen, A.S. Influence of Different Technologies on Dynamic Pricing in District Heating Systems: Comparative Case Studies. *Energy* **2018**, *153*, 136–148. [CrossRef]
46. Loesch, M.; Hufnagel, D.; Steuer, S.; Fabßnacht, T.; Schmeck, H. Demand Side Management in Smart Buildings by Intelligent Scheduling of Heat Pumps. In Proceedings of the 2014 IEEE International Conference on Intelligent Energy and Power Systems, IEPS, Kyiv, Ukraine, 2–6 June 2014; pp. 209–214. [CrossRef]
47. Coelho, A.; Iria, J.; Soares, F.; Lopes, J.P. Real-Time Management of Distributed Multi-Energy Resources in Multi-Energy Networks. *Sustain. Energy Grids Netw.* **2023**, *34*, 101022. [CrossRef]
48. Yan, X.; Ozturk, Y.; Hu, Z.; Song, Y. A Review on Price-Driven Residential Demand Response. *Renew. Sustain. Energy Rev.* **2018**, *96*, 411–419. [CrossRef]
49. Osiadacz, A.J.; Chaczykowski, M. Modeling and Simulation of Gas Distribution Networks in a Multienergy System Environment. *Proc. IEEE* **2020**, *108*, 1580–1595. [CrossRef]
50. EN ISO 52000-1:2017. Available online: http://store.uni.com/catalogo/en-iso-52000-1-2017?josso_back_to=http://store.uni.com/josso-security-check.php&josso_cmd=login_optional&josso_partnerapp_host=store.uni.com (accessed on 6 May 2021).

51. UNI/TS 11300-4:2016—UNI Ente Italiano Di Normazione. Available online: <https://store.uni.com/en/uni-ts-11300-4-2016> (accessed on 9 January 2023).
52. Grossi, I.; Dongellini, M.; Piazzini, A.; Morini, G.L. Dynamic Modelling and Energy Performance Analysis of an Innovative Dual-Source Heat Pump System. *Appl. Therm. Eng.* **2018**, *142*, 745–759. [[CrossRef](#)]
53. Database, M. Meteonorm Version 8—Meteonorm (En). Available online: <https://meteonorm.com/en/meteonorm-version-8> (accessed on 4 March 2021).
54. Pipiciello, M.; Caldera, M.; Cozzini, M.; Ancona, M.A.; Melino, F.; Di Pietra, B. Experimental Characterization of a Prototype of Bidirectional Substation for District Heating with Thermal Prosumers. *Energy* **2021**, *223*, 120036. [[CrossRef](#)]
55. Dino, G.E.; Catrini, P.; Piacentino, A.; Palomba, V.; Frazzica, A. Modelling of a Prosumer’s Substation in a District Heating Network: Validation and Dynamic Analysis. In Proceedings of the 17th SDEWES Conference, Paphos, Cyprus, 6–10 November 2022; pp. 1–15.
56. Kroll. Available online: <http://www.Kroll.de/En/High-Temperature-Heat-Pump-Kwp/> (accessed on 17 December 2022).
57. Kuboth, S.; Heberle, F.; Weith, T.; Welzl, M.; König-Haagen, A.; Brüggemann, D. Experimental Short-Term Investigation of Model Predictive Heat Pump Control in Residential Buildings. *Energy Build.* **2019**, *204*, 109444. [[CrossRef](#)]
58. D’Ettorre, F.; Conti, P.; Schito, E.; Testi, D. Model Predictive Control of a Hybrid Heat Pump System and Impact of the Prediction Horizon on Cost-Saving Potential and Optimal Storage Capacity. *Appl. Therm. Eng.* **2019**, *148*, 524–535. [[CrossRef](#)]
59. Lee, Z.; Gupta, K.; Kircher, K.J.; Zhang, K.M. Mixed-Integer Model Predictive Control of Variable-Speed Heat Pumps. *Energy Build.* **2019**, *198*, 75–83. [[CrossRef](#)]
60. Dino, G.E.; Palomba, V.; Nowak, E.; Frazzica, A. Experimental Characterization of an Innovative Hybrid Thermal-Electric Chiller for Industrial Cooling and Refrigeration Application. *Appl. Energy* **2021**, *281*, 116098. [[CrossRef](#)]
61. Teleriscaldamento Tariffe e Costi in Veneto. Available online: https://www.ilteleriscaldamento.eu/teleriscaldamento_veneto.htm (accessed on 2 February 2023).
62. Giunta, F.; Sawalha, S. Techno-Economic Analysis of Heat Recovery from Supermarket’s CO2 Refrigeration Systems to District Heating Networks. *Appl. Therm. Eng.* **2021**, *193*, 117000. [[CrossRef](#)]
63. Autorità di Regolazione per Energia Reti e Ambiente. Available online: <https://Bolletta.Arera.It/Bolletta20/Index.Php/Guida-Voci-Di-Spesa/Elettricit> (accessed on 8 January 2023).

Disclaimer/Publisher’s Note: The statements, opinions and data contained in all publications are solely those of the individual author(s) and contributor(s) and not of MDPI and/or the editor(s). MDPI and/or the editor(s) disclaim responsibility for any injury to people or property resulting from any ideas, methods, instructions or products referred to in the content.